

**EFFECT OF THERMAL ENERGY ON THE FILLING TIME
OF COMPOSITE ENCAPSULANT UNDERFILLING
PROCESS WITH VARIOUS FILLER LOADING OF NANO
SILICA FILLER PARTICLES**

By:

AMRU ZULKURNAIN

(Matrix no.: 125004)

Supervisor:

DR. MOHAMAD AIZAT ABAS

May 2018

This dissertation is submitted to
Universiti Sains Malaysia
As partial fulfilment of the requirement to graduate with honors degree in
BACHELOR OF ENGINEERING (MECHANICAL ENGINEERING)



UNIVERSITI SAINS MALAYSIA

School of Mechanical Engineering
Engineering Campus
Universiti Sains Malaysia

DECLARATION

I hereby declare that I carried out the reported project in School of Mechanical Engineering, Universiti Sains Malaysia (USM), under the supervision of Dr. Mohamad Aizat Abas. I solemnly declare that to the best of my knowledge, none of this report section has been submitted here or elsewhere in the previous application of degree title. All sources of knowledge used in this report have been duly acknowledged.

.....

Amru Zulkurnain
Matrix No: 125004
Date:

.....

Dr. Mohamad Aizat Abas
Supervisor Date:

ACKNOWLEDGMENT

The highest gratitude goes to the God for giving me a good health and wellbeing along the venture of final year project completion. It was a tough journey and required a lot of sacrifices but by the wisdom from Him, I managed to withstand through it successfully.

I also would like to express my deepest appreciation to my final year project supervisor, Dr. Mohamad Aizat Abas, for giving me the opportunity and encouragement to conduct project under his supervision. Persistent help and guidance from him have given me a clear vision and solution on the completion of the project, thus, made it possible for me to achieve as best as I could in the project.

In addition, my sincere thank you to Fei Chong Ng., Universiti Sains Malaysia (USM) postgraduate students for assisting me through the project completion. Lots of knowledge was gained by the sharing of expertise regarding to the project in the solution findings to tackle the occurred problems.

Lastly, I would like to thank my family and friends for supporting me spiritually and physically throughout the project and my life in general. It elevated my spirit to work continuously and achieve for the best for the final project of my studies.

CONTENTS

DECLARATION	i
ACKNOWLEDGMENT	ii
CONTENTS.....	iii
LIST OF TABLES	iv
LIST OF FIGURES	v
LIST OF ABBREVIATIONS.....	vi
ABSTRAK.....	vii
ABSTRACT.....	viii
CHAPTER 1	1
INTRODUCTION.....	1
1.1 Overview	1
1.3 Objective.....	3
1.4 Scope of Project.....	4
CHAPTER 2	5
LITERATURE REVIEW	5
CHAPTER 3	7
METHODOLOGY	7
3.1 Experimental Procedure.	7
3.2 Numerical simulation.	11
CHAPTER 4	17
RESULTS AND DISCUSSIONS	17
4.1 Experimental validation.....	17
4.2 Filling time	21
4.3 Thermal Energy	26
4.4 Filler accumulation and swirling	27
CHAPTER 5	28
CONCLUSION.....	28
REFERENCE.....	29

LIST OF TABLES

Table 3. 1 Dimension of scale up 10×10 of BGA model as compare to actual industrial BGA model.....	7
Table 3. 2. Show the parameter of BGA model used for FVM-DPM simulation.....	11
Table 3. 3 Show the effect of grid resolution and number of cells velocity and pressure of 15wt% filler loading	12
Table 4. 1 Experimental and simulation filling time (0.05 wt% of filler particles) at difference filling percentage with influence of thermal energy at 60 °C.....	17
Table 4. 2 Experimental and simulation filling time (0.05 wt% of filler particles) at difference filling percentage with influence of thermal energy at 80 °C.....	18
Table 4. 3 Experimental and simulation filling time (0.05 wt% of filler particles) at difference filling percentage with influence of thermal energy at 100 °C.....	18
Table 4. 4 Experimental and simulation filling time (5 wt% of filler particles) at difference filling percentage with influence of thermal energy at 60 °C.....	19
Table 4. 5. Experimental and simulation filling time (5 wt% of filler particles) at difference filling percentage with influence of thermal energy at 80 °C.....	19
Table 4. 6. Experimental and simulation filling time (5 wt% of filler particles) at difference filling percentage with influence of thermal energy at 100 °C.....	20
Table 4. 7. Flow front of mixture of encapsulant and 5 wt% filler particles through BGA model at difference thermal energy.....	22
Table 4. 8 Filling time of 5 wt% filler loading at difference thermal Energy.....	23
Table 4. 9. Flow front of mixture of encapsulant and 10 wt% filler particles through BGA model at difference thermal energy.....	23
Table 4. 10 Filling time of 10 wt% filler loading at difference thermal Energy	24
Table 4. 11. Flow front of mixture of encapsulant and 15 wt% filler particles through BGA model at difference thermal energy.....	25
Table 4. 12 Filling time of 15 wt% filler loading at difference thermal Energy.....	25

LIST OF FIGURES

Fig 3. 1 Show the bumps diameter, bumps pitch and bumps height	8
Fig 3. 2 The side view of the BGA model.	8
Fig 3. 3 The isometric view of the BGA model.....	8
Fig 3. 4 Showside by side the schematic diagram of the flow system and experimental set-up	10
Fig 3. 5 (a) show the BGA model used in the experiment, (b) is the electrical stove to introduce thermal energy (c)oil bath and LED lighting attached.....	10
Fig 3. 6 Difference grid resolution for BGA model. (1-Course, 2-Medium, 3-Fine, 4-Fine), that used for grid resolution test.....	13
Fig. 4. 1 Experiment (Exp) and simulation (Sim) results of filling time against filling percentages for 0.05 wt% filler particles	20
Fig. 4. 2 Experiment (Exp) and simulation (Sim) results of filling time against filling percentages for 5 wt% filler particles	21
Fig. 4. 3. Show the effect of thermal energy to the filling time of 5 wt% filler loading.	23
Fig. 4. 4. Show the effect of thermal energy to the filling time of 10 wt% filler loading.	25
Fig. 4. 5. Show the effect of thermal energy to the filling time of 15 wt% filler loading.	26
Fig. 4. 6. Show the asymmetry of the encapsulant flow at higher thermal energy.	26
Fig. 4. 7. Filler accumulation and swirling in the underfilling process using the 5 wt% filler loading at 100 °C thermal energy.	27

LIST OF ABBREVIATIONS

Nomenclatures	Descriptions
IC	Integrated circuit
FVM	Finite volume method
DPM	Printed circuit board
PCB	Ball grid array
BGA	Thermal expansion
SiO ₂	Nano-Silica
VOF	Volume of fluid

ABSTRAK

Kemajuan komposit encapsulant dengan partikel pengisi pengukuh dalam resin epoxy adalah suatu revolusi penambahbaikan dalam cubaan untuk membantu kebolehpercayaan alatan elektronik. Banyak kajian telah membuktikan dengan menambah kuantiti partikel pengisi dalam komposit encapsulant, kebolehpercayaan dan kemampuan litar bersepadu meningkat. Dengan meningkatkan kuantiti partikel pengisi dalam encapsulant jelas menunjukkan peningkatan masa pengisian. Ini dipercayai disebabkan penambahan kuantiti partikel pengisi menyebabkan encapsulant menjadi likat. Dalam kajian ini, permasalahan ini diselesaikan dengan menambah tenaga haba semasa proses mengisi. Dalam kajian ini juga, kaedah simulasi dan eksperimen dilakukan untuk mengkaji kesan tenaga haba kepada masa pengisian dengan menggunakan variasi kuantiti partikel pengisi. Bagi simulasi, kaedah jumlah terhingga berdasarkan penyelesaian berangka dengan menggunakan model fasa diskret. Berdasarkan keputusan simulasi dan eksperimen, membuktikan yang tenaga haba mampu mengurangkan masa pengisian bagi proses pengisian antara kuantiti zarah pengisi yang berbeza dengan purata 5%.

ABSTRACT

The advance composite encapsulant with reinforce filler particle in the epoxy resin is a revolutionary advancement in the effort to improve the reliability of the electronic device. Many researches have been shown that by increase the amount of the filler particles in the composite encapsulant, the reliability and sustainability of the integrated circuit (IC) is improved. The introduction of higher amount of filler particles in the encapsulant in turn increasing the filling time of the underfilling process significantly. It has been found that the higher filler loading causing the encapsulant to become more viscous. In this research, straight forward solution to this is by incorporating additional energy during the underfilling process. In this research, simulation and experimental analysis is conducted to study the effect of thermal energy to the filling time of composite underfilling time at different filler loading. For simulation, finite volume method (FVM) based numerical solver using discrete phase model (DPM). From simulation and experimental results, it is proven that the thermal energy is able to reduce the filling time of the underfilling process between difference filler loading by average of 5%.

CHAPTER 1

INTRODUCTION

1.1 Overview

Technology world create a rush in the electronic industries for smaller yet compact electronic components, this urge the electronic company to develop miniature integrated circuit (IC). However, the reduction in size of IC is a challenge task for industry to deal with the interconnection joints between the IC package and printed circuit board (PCB). Alternatively, ball grid array (BGA) is introducing to overcome the limitation of the previous interconnection joint, as BGA able to densely packed interconnection joint array with better strength joint and overall heat dissipation [1,2]. However, due to difference coefficient of thermal expansion (CTE) of solder ball and the silicon chip, causing thermal stress within the package. Hence, the reliability of the package will be reduced. To overcome this underfilled encapsulant process is invented to fill the void space between IC package and PCB with controlled amount of electrically-insulated adhesive mould. The underfilled encapsulant will serve as physical protection of roller ball from contamination and able to distribution thermomechanical stress within the package.

While the problem of the pin joint connection being solve, the optimization of the underfill encapsulant procedure in electronic packaging process is still represent an uphill battle. For instant, issues relating to incomplete filling, void formation [5] and reverse flow [6]. Many research have been conducted in past decade to optimize the underfill process based on difference design parameter and underfilling condition, such as the solder bump arrangement [7,8], gap height [9], inlet pressure [11] and silicon chip thickness [12].

Most of the listed literature [5-13] attempted to improve and optimize the underfilling encapsulation process of flip chip device by considering different operating conditions of the underfill process on packaging designs. The study is limited to the improvement of the material of the encapsulant being used. Generally, the reliability of the encapsulated packaging relied on both nature and quality of the encapsulant. There is an advance underfilled material that relied heavily on introduction of well- dispersed inorganic particles into the polymer resin. This underfilled material is known as filler-filled composite encapsulant which had been patented as early as in the year 2002 [14,15]. The most common

commercially available composite encapsulant used in the industries is the mono-dispersed nano-silica (SiO_2). The infusion of the filler particle into the resin proven to increase the tensile strength of the polymer composite while the same time reduce the CTE [14,17]. The low CTE increase the reliability of the package by reducing the thermal stress. Apart from the underfilling encapsulant sector, the additive of metallic filler particles in the solder paste is a common practice in soldering field to enhance reliability of the solder paste joint [8-20].

As the technology grow significantly fast, electronic company is pressured to supply the demand for the electronic component. Now industries are looking for developing the processing method that able to reduce the processing time. As the primary driving force of conventional underfilling flow is the capillary motion, few research have been attempted to promote the flow by increasing the driving force. Due to this issue, several variations of underfill process had been introduced, for instance, vacuum-assisted, raised-die [4], thermocapillary [6], and pressurized [13]. Research on the effect of temperature to the capillary flow to the underfill flow had been done [6]. The study however is limited since no study have been done on the effect of the temperature on the underfilled BGA using nano silica filler reinforce composite encapsulant. From the previous research [6] the flow time of the underfill is proven to be improve by introducing temperature to the process. This issue originates from insufficient energy or capillary force of the encapsulant. The increase in thermal energy can be introduce by preheating the top of the PCB through controlled force convection, commonly known as hot air bath.

To the best knowledge of the authors, no research has been found to study the effect of thermal energy on the underfilled BGA using nano silica filler reinforce composite encapsulant in term of its filling time, thermal, velocity and pressure distribution. Majority of the research on the encapsulation process were focused on flow pattern, effect of filler-filled and pressure distribution only with constant thermal distribution. To enhance the validity of the current study, both numerical simulation and experimental observation will be conducted to investigate the effectiveness of thermal energy in improving the total filling time of the underfill using nano silica filler reinforce composite encapsulant.

1.2 Problem Statement

Recent trend in electronic industries are demanding smaller chip packaging process along with increase in performance and reliability of the package. The introduction of Ball Grid Array (BGA) is a game changer in production of electronic chip. Due to the different coefficient of thermal expansion (CTE) of the solder balls to the substrate and silicon chip, thermal mismatch will occur and give rise to the thermal stress in the package. Introduction of underfill encapsulation process is carried out as part of the electronic packaging procedures to overcome the issue. However, the industrial encapsulant being used does not have high tensile strength and poor CTE [14-17]. Thus, nano-silica filler particle is infused into encapsulant to improve the tensile strength and reduce the CTE, upon considering the fact that the increase in filler loading of composite-encapsulant may further enhance the packing reliability as proven by Vincent et al. (2004). Unfortunately, due to increase the weight percentage nano-silica filler particle the composite's viscosity increase which resulting to longer encapsulation process [21]. In this study, thermal energy will be introduced during the encapsulation process to reduce the duration of encapsulation process. The thermal energy is introduced to PCB through hot plate which is placed under the PCB.

1.3 Objective

The objectives of this project are as follows:

1. To determine the flow rate of the composite-encapsulant during the underfill process.
2. To determine the distribution of the nano-silica filler particle in the composite-encapsulant.
3. To improve the flow rate of the composite-encapsulant during underfill process by introducing thermal energy.

1.4 Scope of Project

An experiment is conducted based on the effect of thermal energy on the filling time of composite encapsulant underfilling process on BGA using 8 time scale up model with various filler loading of nano silica filler particle. A simulation with the scale up version of BGA model is conducted to verify the experimental data. Besides, the simulation with the scale up version of BGA also serve to verify the methodology of the FVM-DPM simulation setup. Next, the simulation is tested through real scale of BGA model same as the dimension that used in the industries. The data obtain is analysed to prove the hypnotists of this study.

CHAPTER 2

LITERATURE REVIEW

Research on electronic circuit is a very active research around the globe due to high demand in the technology era especially for the IC. Challenge keep arise in this field specially to miniature electronic component. The key factor is to make the component compact while serve better. This give rise to development of BGA to simplify the joint connection between IC and PCB. Which is better strength joint and better overall heat dissipation [1,2]. However, it BGA still representing uphill battle such ass difference CTE between solder ball and silicon chip causing thermal stress in the package. Thus, researcher design underfill encapsulant to overcome the problem. This method still need huge improvement, for instant issues relating to void formation [5], incomplete filling and reverse flow [6]. Most listed literatures [5-13] try to improve and optimize the underfilling encapsulant process, however limited amount of study is done to improve the encapsulant being used. There is advance underfill material which introduce well dispersed inorganic particles into the encapsulant in early as the year 2002 [14,15].

There is research done by Ng et al. (20016) to study the effect of filler filled amount on the effect of the encapsulant flow during underfill process. The research is done for IC device with 10×10 BGA interconnection joint between PCB layer. The filler is measure in weight percentage (wt%) is varied for each underfilling cases. Accordingly, five difference values of filler loading will be chosen in the study which can be divided into two classes: low filler loadings (2 wt% and 5 wt%) and high filler loading (15 wt%, 20wt% and 25wt%)it is not worthy to mention that all the chosen filler loading are lower than 30wt% since research has shown that beyond this concentration, the composite's viscosity increase exponentially thereby reducing the filler time substantially [21]. From this research

In terms of the filling time, flow-ability, particle accumulation and filler collision, it is concluded that both 2 wt% and 5 wt% are the optimum nano-silica filler loadings, since no issues were being observed. This is because at low filler loadings, the low amount of nano-silica dispersed is unable to significantly alter the flow behaviour, thus comparable to the underfilling flow of pure encapsulant. Upon considering the fact that the increase in filler loadings of composite-encapsulant may further enhance the packaging reliability, the 15 wt% composite-encapsulant is eventually the recommended filler loading, since its flow behaviour

is not prominently affected by the nano-silica fillers dispersed. On contrary, at higher filler loadings such as 20 wt% and 25 wt%, slow yet asymmetry underfilling flow are attained together with potential particle accumulation and high solder ball erosion. The productivity of encapsulation process may become lower due to the prolonged lead time and possible occurrence of defects, such as incomplete filing and void formation. The reliability of solder ball might also be slightly affected due to high collision rate.

Hence, to the best knowledge of authors, there is study on the effect of thermal energy on the composite-encapsulant flow during the underfill process. But there is a study on the effect of thermocapillary action in the underfill encapsulant of multi-stack ball grid array [6]. From the study, a straightforward solution by incorporating additional thermal energy in the encapsulant to increases its flowability is introduced. This additional thermal energy at the upper layer produces a distinct temperature difference between the upper and lower layers, or simply thermal delta. This research attempts to demonstrate the effectiveness of thermal delta in solving the flow problem during encapsulation process of multi-stacks BGA. The findings have shown that the experimental data compares well with the simulation results. It was also found that the implementation of thermal delta substantially reduces the filling time across the multi-stack packages. This study reveals the potential of thermocapillary-driven underfill encapsulation. It has also been found that the encapsulant lacks energy to flow at the upper layer due to lower hydrostatics pressure.

Thus, the focus of this study is to improve the filling time of underfilling process using the nano-silica filler composite-encapsulant. Through this study packaging reliability able to be maintain at optimum while reducing filling time.

CHAPTER 3

METHODOLOGY

3.1 Experimental Procedure.

3.1.1 Establishment of computer aided design (CAD) model.

The CAD model in this project is model by the 10 x 10 BGA model with the scaling up dimension. Scale up is required due to the limitation of the experimental instrument to handle very small dimension of actual industrial BGA model. The model is scale up to 8 time the real scale of the BGA model. 100 BGA ball is represent solder ball in actual IC is arranged in rectangular array by 10 solder ball in a row. The BGA is sandwich together by two PCB.

Three-dimension CAD model of scale up BGA model is constructed using Solidwork software. The dimension of the BGA model is illustrated in table 3.1. The BGA model will be place in housing which look like a tub. The housing consists two walls at the side which act as barrier and front and back of the BGA model. The side barrier is to prevent the encapsulant to spilled to the side due to low hydrostatic pressure. The implementation of barrier is also practise by electronic manufacturing company. The housing will prevent the mixing of oil from oil bath with composite glycerine and hollow glass spheres. The housing has the dimension of 140mm in length, weight of 96mm and height 50mm.

Parameter	Actual Model	Scale up Model
PCB/Plate (mm)	Not applicable	92(L) × 92(w) × 7.6
Bump Diameter (mm)	0.5	4.0
Bump Pitch (mm)	1.0	8.0
Bump Height (mm)	0.45	3.6

Table 3. 1 Dimension of scale up 10 × 10 of BGA model as compare to actual industrial BGA model.

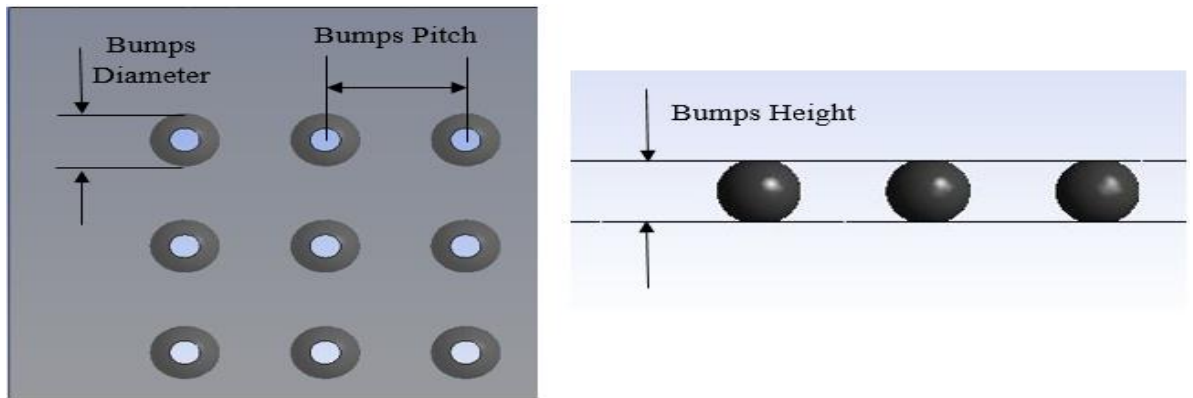


Fig 3. 1 Show the bumps diameter, bumps pitch and bumps height

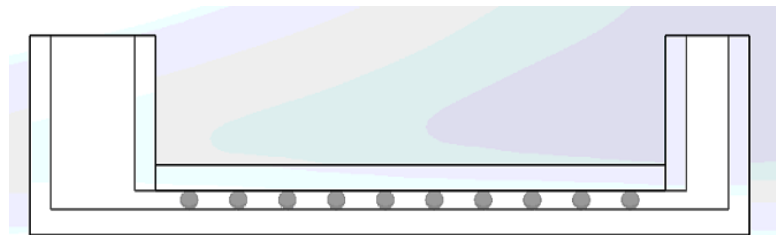


Fig 3. 2 The side view of the BGA model.

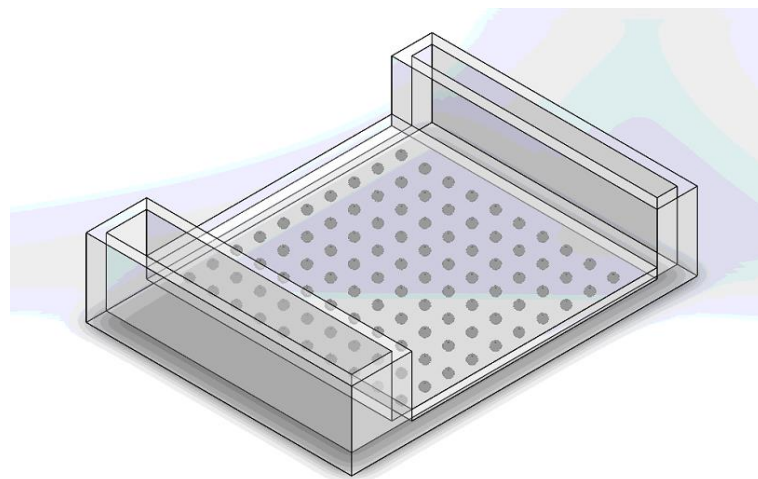


Fig 3. 3 The isometric view of the BGA model

3.1.2 Fabrication of experimental model

CAD drawing is prepared based on the three-dimension BGA model and housing. The dimension is transferred to 2mm thick Perspex to be cut. The parts that has been cut is assemble and glue using chloroform. Plastic bead that has diameter of 4mm and height of 3.6mm is used to represent BGA in BGA model.

3.1.3 Experimental setup and procedure.

The particle image velocimetry (PIV) experiment is setup in aerodynamic lab in School of Aerospace. The flow system is illustrated in fig. 3.4 in the schematic diagram, wire connection is indicated by black lines, the inlet is the place where composite glycerine and hollow glass spheres is dispensed and the outlet is the flow of composite glycerine and hollow glass spheres will end.

In this setup the fluid that will be using is glycerine which will be add with hollow glass spheres (HGS) of 10 micro meters in diameter. The HGS will act as filler particles in real encapsulant and as particle tracker for PIV measurement system. In this setup, weight percent (wt%) of HGS will be varied from 0.05wt% and 5 wt%; the variation weight percent of HGS is to mimic the filler loading in real composite encapsulant. The 0.05 wt% of HGS is to represent zero wt% filler loading of real composite encapsulant, this is because the PIV measurement system unable to perform the measurement without the particle tracker. This experiment is limited to two weight percent compared to three weight percent in this research, due to the cost of operation is very high and not relevant.

Light emitting diode (LED) will be used to illuminate the hollow glass sphere during the fluid flow. The hollow glass sphere is manufacture by coating the particles with silver coated which design to shine to light source. The LED will be mount to the side of the BGA model as shown in the setup.

The BGA model will be submerged in the oil bath throughout the underfill process. The oil bath will be heated with electrical stove to desired temperature which is 60°C, 80°C and 100°C. Throughout underfilling process the temperature will be keep constant; thermocouple will be dip into the oil bath to monitor the temperature.

The camera Canon D100 with lens of 18mm – 55mm f/3.5 will be using to record the video of the fluid flow. This camera has maximum frame rate of 60 frame per second. Image of the flow will be extracted by frame to be analysed in the PIV solver in MathLab software.

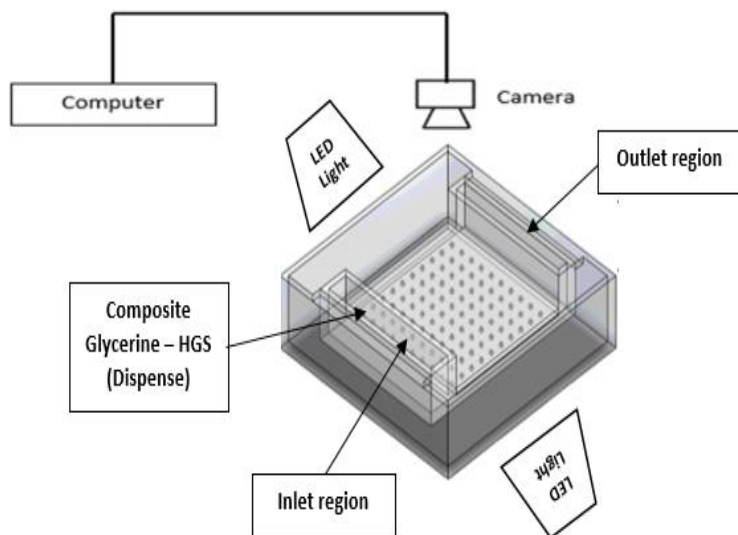
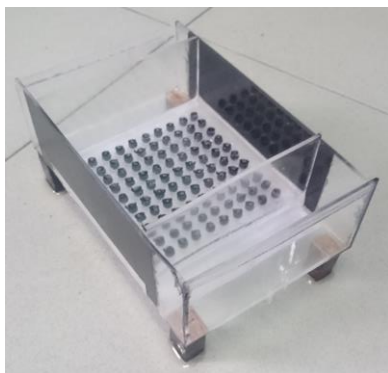


Fig 3. 4 Showside by side the schematic diagram of the flow system and experimental set-up



(a)



(b)



(c)

Fig 3. 5 (a) show the BGA model used in the experiment, (b) is the electrical stove to introduce thermal energy (c)oil bath and LED lighting attached.

3.2 Numerical simulation.

In this research finite volume method (FVM) is being utilized to simulate the capillary underfill encapsulant process of ball grid array (BGA) through Ansys Fluent software. In this simulation, three-dimensional multiphase model, dispersed phase model (DPM) and laminar model are run together. In this section explaining about geometrical mesh generation, mathematical model, boundary condition and numerical solver.

Numerical geometrical model of BGA is build based on the 10 x 10 BGA of printed circuit board (PCB) that is being used by the industries. The detail about the BGA model is describe is table 2. In this simulation, the flow front progression of mixture of encapsulant with filler particle will be simulated as the mixture is dispense normally at the inlet surface as it flows toward the outlet.

Parameter	
PCB/ Parallel Plates (mm)	10.5 x10.5 x 3.5
Bump Height (mm)	0.5
Bump Pitch (mm)	1.0
Bump Diameter (mm)	0.45
Number of solder ball	100

Table 3. 2. Show the parameter of BGA model used for FVM-DPM simulation

3.2.1. Mesh Generation.

Mesh is one of the biggest factor in determining the cost of simulation. Finest mesh will provide good and accurate result; however, it will cost huge time for simulation. So, the optimum mesh size need to be choose by considering the cost and accuracy of the simulation. Optimum mesh size is obtained through grid independent test, where course, medium, fine and finest mesh sizes is tested based on selected variables and the error that produce. The results of grid independent test are shown in table 3.6. From the result obtain, this showed that numerical results are invariant based on the grids size and cell number. Mesh sizes of model 3 is chosen for the mesh geometry that will be used in the simulation.

Path – conforming tetrahedral mesh technique is selected to model the mesh for the fluid domain of BGA model. The density of mesh cell near the solder ball are design to be higher than in elsewhere; higher density mesh model able to compute more accurate integration of fluid flow near the solder ball. Besides, the equal – size of skewness is maintained to be less than 0.8 benchmark [24]. This simulation is optimized based on methodology outlined by Aizat et. Al [25] to obtain the most precise mesh geometry.

Through discrete phase method, particle is not track individually as particle size ($d_p = 10 \text{ e}^{-7} \text{ m}$) is less than average mesh size ($d_m = 10 \text{ e}^{-5} \text{ m}$), where $\frac{d_p}{d_m} \sim 100$. Thus, DPM track the particle in parcel rather than individual as it is impossible and very costly. Each parcel is identified by the group of particles that has same physical properties along the trajectory, which contain around 1,000 – 100,000 particles. In DPM the mass flow rate and the time step requirement is determine by the motion of the particle [23,24].

Mesh models	Grid resolution	Number of nodes	Number of cells	Gauge Pressure (Pa)	Discretization error (%)	Velocity (m/s)	Discretization error (%)
1	Coarse	33,920	147,470	4085.14	0.512	0.001307	3.362
2	Medium	89,607	419,518	4100.76	0.237	0.001298	2.471
3	Fine	134,692	623,663	4119.62	0.021	0.001224	0.626
4	Fine	146,149	674,280	4120.01	-	0.001218	-

Table 3. 3 Show the effect of grid resolution and number of cells velocity and pressure of 15wt% filler loading

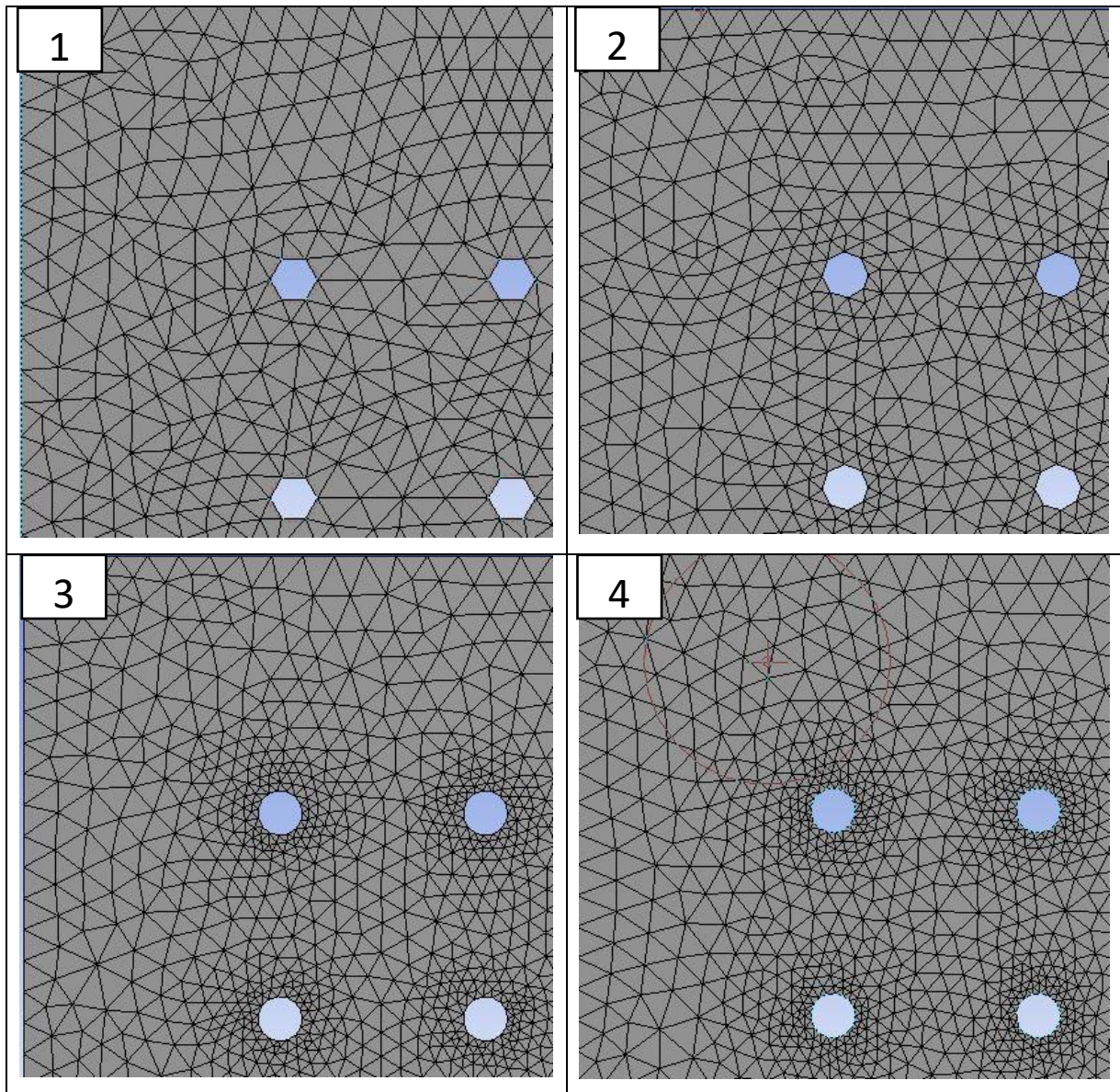


Fig 3. 6 Difference grid resolution for BGA model. (1-Course, 2-Medium, 3-Fine, 4-Fine), that used for grid resolution test.

3.2.2. Mathematical models and governing equations.

3.2.2.1. Continuous phase.

In finite volume method (FVM), continuity (mass balance) and Navier – Stoke equation determine that three – dimensional Eulerian continuous phase flow of underfill encapsulant to be unsteady, laminar and incompressible.

Continuity equation: $\frac{\partial \rho_f}{\partial t} + \nabla \cdot (\rho_f \vec{u}) = 0$

Navier – Stokes equation: $\frac{\partial}{\partial t} (\rho_f \vec{u}) + \nabla \cdot (\rho_f \vec{u} \cdot \vec{u}) = -\nabla p + \nabla \cdot \vec{\tau} + \rho_f \vec{g}$

ρ_f = Fluid density

\vec{u} = velocity vector of fluid

P = pressure

τ = Shear stress tensor

\vec{g} = Gravitational acceleration

Moreover, implicit formulation was adopted for volume fraction formulation. The flow is characterised to two fluid phases, where primary phase is air and secondary phase is encapsulant. Primary phase plays important role in the underfilling flow and cannot be neglected. Volume of fluid (VOF) method is used to track the fluid flow of mixture of encapsulant and filler particle. The formulation of VOF is:

$$\frac{\partial}{\partial t} f + \vec{u} \cdot \nabla f = 0, \text{ where } f: \text{ encapsulant's volume fraction; value between 0 or 1}$$

1 ~ region populated with encapsulant

2 ~ region not populated with encapsulant

3.2.2.2. Discrete particle phase.

Nano silica particle's trajectory inside the encapsulant during the dispense is subjected to various type of force, the force balance is express by the Langrangian reference frame. The equation of motion for the particle are:

$$\frac{\partial \vec{x}_p}{\partial t} = \vec{v}_p$$

$$\frac{\partial \vec{v}_p}{\partial t} = F_D (\vec{u} - \vec{v}_p) + \vec{g} \frac{(\rho_p - \rho_f)}{\rho_f} + \vec{F}_L + \vec{F}_{vm}$$

Subscripts “p” refers to properties and the parameter of filler particle. The term $F_D (\vec{u} - \vec{v}_p)$ is corresponding to drag force per unit particle's mass. However, since the particles diameter is considered small which $d_p = 100$ nm. The drag force is described based on the Stokes – Cunningham formulation:

$$F_D = \frac{18\mu_f}{d_p \rho_p C_c}$$

Where, μ_f is dynamic viscosity of encapsulant. Then, C_c is dimensionless Cunningham correction factor:

$$C_c = 1 + \frac{2\lambda}{d_p} \left[1.257 + 0.4 \exp\left(-\frac{1.1d_p}{2\lambda}\right) \right]$$

Where, $\lambda = \frac{1}{\sqrt{2}\pi n d_p^2}$, n is particles number density.

Weight of nano silica particle used in the simulation is relatively very small compared to overall BGA model. Most literature will exclude the effect of gravitational force, however to mimic the real industrial setup, we include the effect of the gravitational in the force balance.

Saffman's lift generation is used to model the lift force per unit particle's mass, F_L . the magnitude of the lift force is

$$|\vec{F}_L| = \frac{2k\sqrt{v_f}\rho_f d_{ij}}{\rho_p d_p (d_{ik} d_{kl})^{\frac{1}{4}}} |\vec{u} - \vec{v}_p|$$

Where dimensionless constant, $k = 2.594$. V_f is fluid kinematic viscosity, Deformation tensor is denoted as d_{ij} , d_{ik} and d_{kl} .

Virtual mass force is an unsteady force due to change in relative velocity of dispense particle and encapsulant fluid. This is due to both particle and encapsulant have comparative density, which are 1150 kg/m^3 and 1300 kg/m^3 .

$$\vec{F}_{VM} = \frac{1}{2} \frac{\rho_f}{\rho_p} \left(\vec{v}_p \cdot \nabla \vec{u} - \frac{d\vec{v}_p}{dt} \right)$$

3.2.3 Boundary condition

Underfill encapsulate is dispense continuously at the inlet surface at the rate of 1.8 mm/s which is the speed of the injection used by industries. At the mean time nano silica particle is injected perpendicularly at the inlet surface. The speed of the nano silica particle is set to zero as the particle is assumed to be carried along by the continuous phase flow of encapsulant.

The conventional no slip boundary condition is applied for all wall in fluid domain. For inlet and outlet, escape boundary condition is applied to allow the continuous fluid flow. Reflect boundary condition is set at solder ball, side wall and top and bottom plates. Pressure at outlet is set to be at constant atmospheric pressure.

In this study, whole underfill encapsulant process is influenced by thermal energy. Since, thermal energy is one of the manipulated variables in these studies. To satisfy the thermal energy, energy equation is applied in this simulation. Whole BGA model including solder ball, side wall, top and bottom plates is set to respective manipulated variable temperature. The respective temperature also implies on the continuous phase flow at the inlet.

3.2.4 Numerical solution.

Simple algorithm scheme is implied in this simulation to couple the velocity and pressure. Next, second – order upwind scheme is adopted to increase the accuracy of the simulation. Implicit solver is used for multiphase VOF model to reduce the computational time. The optimum time step of 0.2 second with 1,000 step sizes is used in this simulation.

CHAPTER 4

RESULTS AND DISCUSSIONS

4.1 Experimental validation.

This section shows chases of filler loading of 0.05 wt % and 5 wt% is forecast using DPM simulation and experimental analysis to determine the flow front profiles across the BGA at differences filler stages. Table 4 until table 4.5 shown side by side comparison of the flow front of the underfill process. From the result obtain between simulation and experiment is almost identical. The flow progression of underfill by the experiment and the simulation is consistent to what is being reported in most other literature [5-10]. Base on the flow front obtain experiment analysis and simulation on scale up BGA, FVM – DPM methodology that is used for this DPM simulation is robust for future analysis. Detail analysis regarding these validation and comparison will be discuss further in section 4.2, 4.3 and 4.4. Thus, this conclude that current numerical methodology is capable to model the encapsulant underfill process for BGA model.

Table 4. 1 Experimental and simulation filling time (0.05 wt% of filler particles) at difference filling percentage with influence of thermal energy at 60 °C


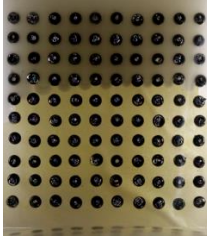
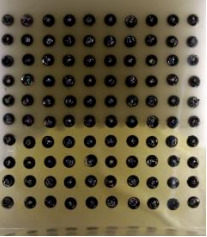
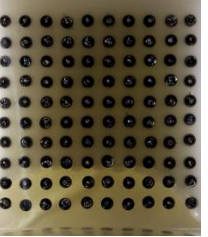
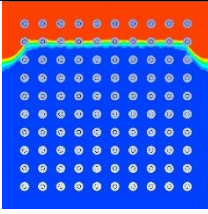
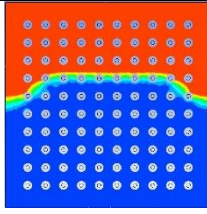
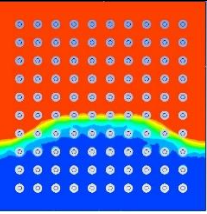
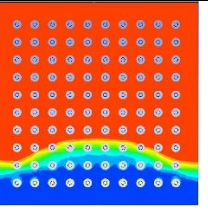
	Filling percentage (%)			
	20	40	60	80
Experimental				
Simulation				
FVM – DPM filling time				
Experiment (s)	9	24	39	77
Simulation (s)	13	22	45	80

Table 4. 2 Experimental and simulation filling time (0.05 wt% of filler particles) at difference filling percentage with influence of thermal energy at 80 °C

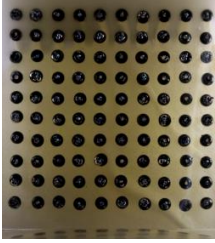
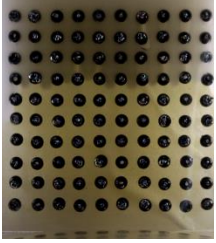


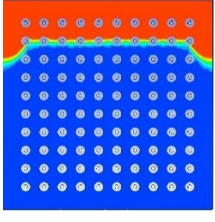
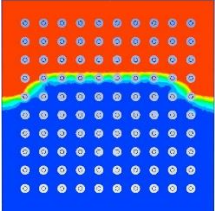
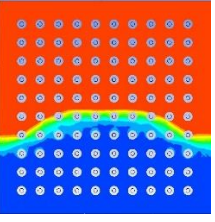
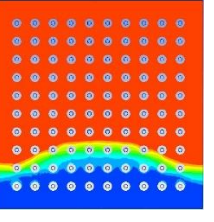
	Filling percentage (%)			
	20	40	60	80
Experimental				
Simulation				
FVM – DPM filling time				
Experiment (s)	6	18	33	65
Simulation (s)	8	16	34	67

Table 4. 3 Experimental and simulation filling time (0.05 wt% of filler particles) at difference filling percentage with influence of thermal energy at 100 °C

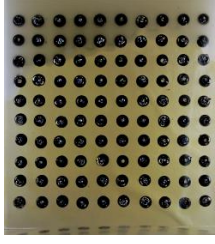



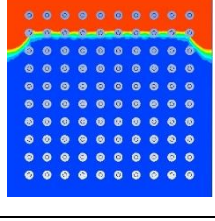
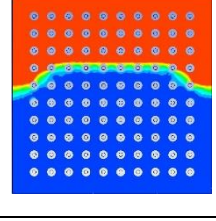
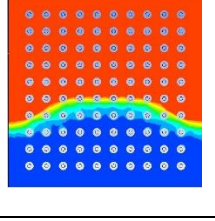
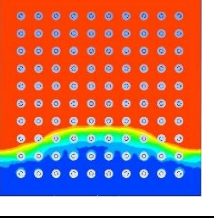
	Filling percentage (%)			
	20	40	60	80
Experimental				
Simulation				
FVM – DPM filling time				
Experiment (s)	4	12	28	51
Simulation (s)	3	10	26	55

Table 4. 4 Experimental and simulation filling time (5 wt% of filler particles) at difference filling percentage with influence of thermal energy at 60 °C.

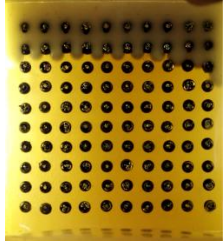
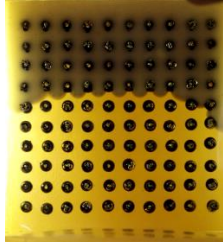
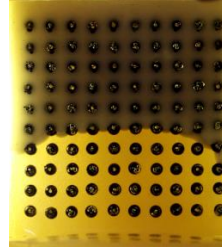
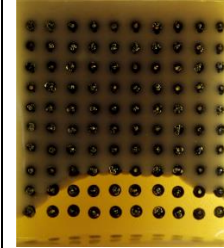
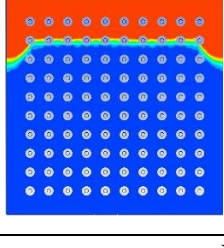
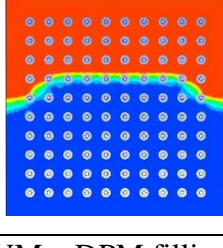
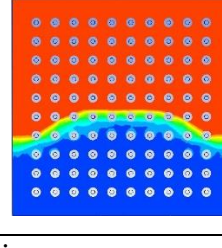
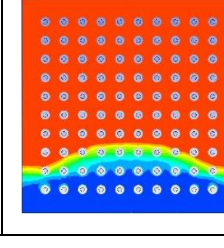
		Filling percentage (%)			
		20	40	60	80
Experimental					
Simulation					
FVM – DPM filling time					
Experiment (s)		17	28	49	84
Simulation (s)		14	26	51	93

Table 4. 5. Experimental and simulation filling time (5 wt% of filler particles) at difference filling percentage with influence of thermal energy at 80 °C

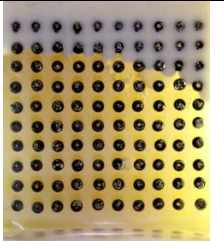
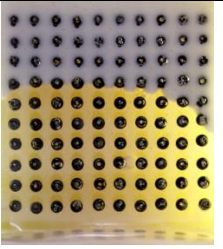
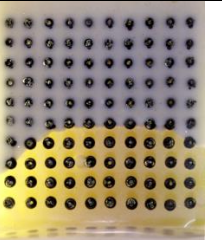
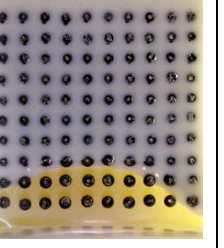
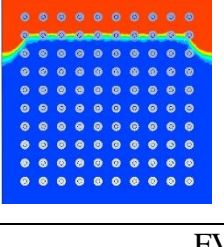
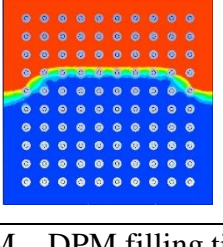
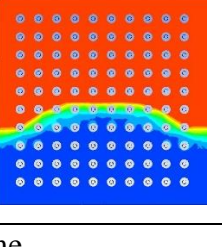
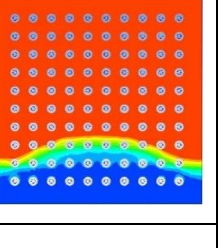
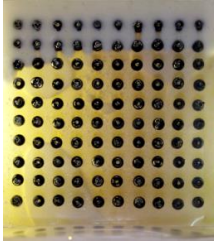
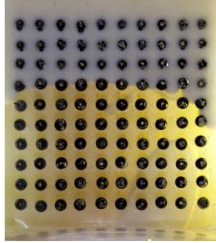
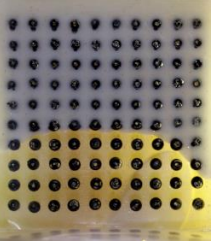
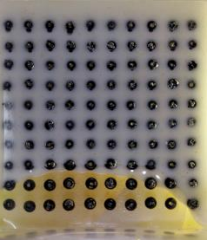
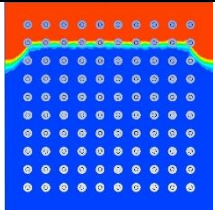
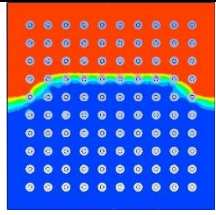
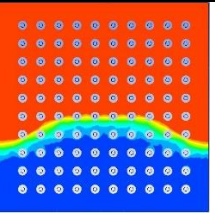
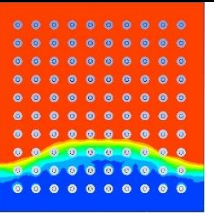
		Filling percentage (%)			
		20	40	60	80
Experimental					
Simulation					
FVM – DPM filling time					
Experiment (s)		13	21	40	71
Simulation (s)		11	20	39	76

Table 4. 6. Experimental and simulation filling time (5 wt% of filler particles) at difference filling percentage with influence of thermal energy at 100 °C

	Filling percentage (%)			
	20	40	60	80
Experimental				
Simulation				
FVM – DPM filling time				
Experiment (s)	9	19	32	63
Simulation (s)	7	11	30	63

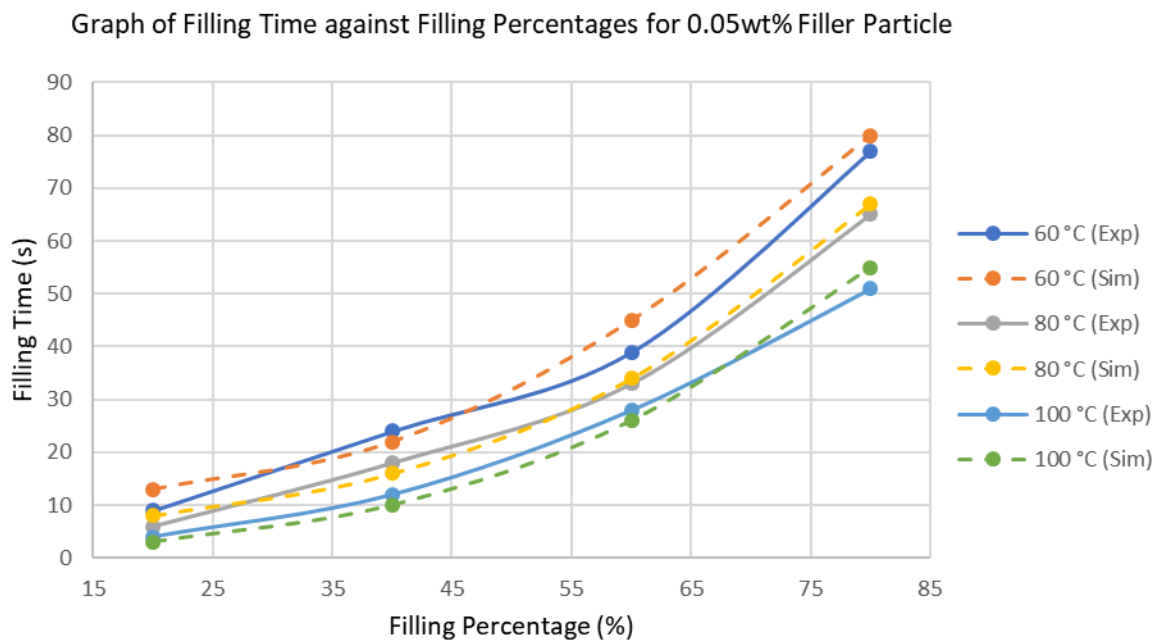


Fig. 4. 1 Experiment (Exp) and simulation (Sim) results of filling time against filling percentages for 0.05 wt% filler particles

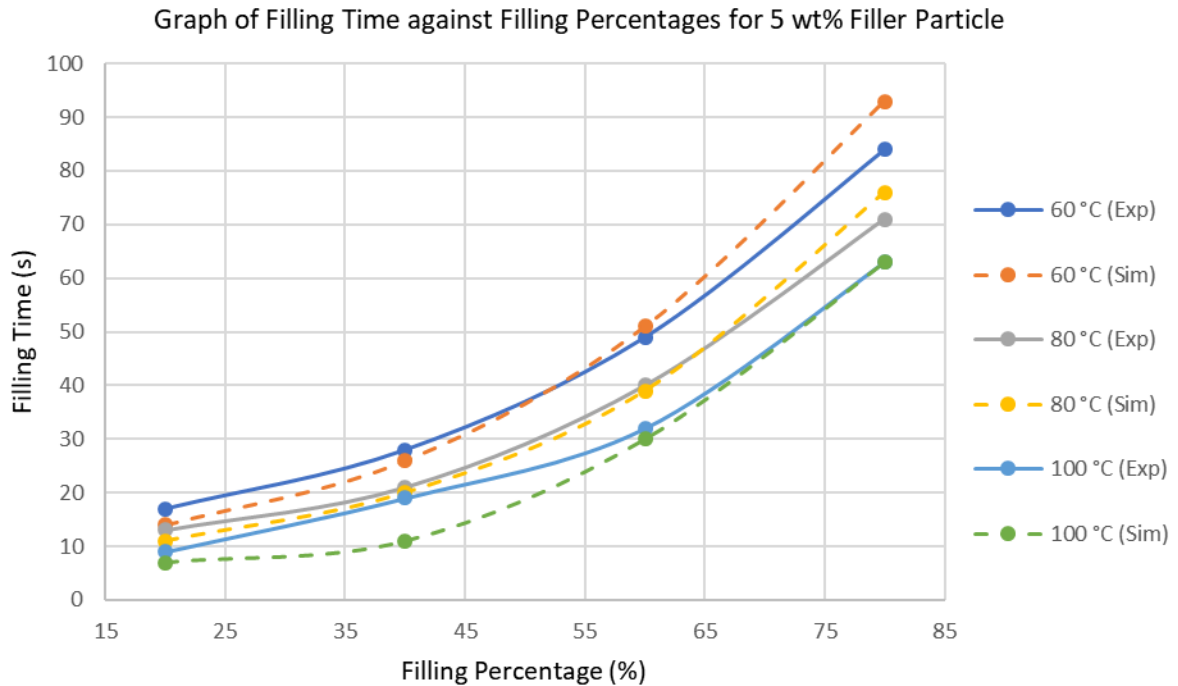


Fig. 4. 2 Experiment (Exp) and simulation (Sim) results of filling time against filling percentages for 5 wt% filler particles

4.2 Filling time

In this section FVM – DPM simulation on effect of thermal energy on the various filler loading is simulated based on the real scale BGA model. In table 4.7, 4.9 and 4.11 show the encapsulant volume fraction at difference thermal energy for respective filler loading. From table 4.8, 4.10 and 4.11, it shows that the filling time of the underfill at every filling stage is increases with the increase of the filler loading. This show that the filler loading is affecting the flow – ability and dynamic of underfill flow. This is due to the filler loading will alter the fluid properties in term of density and viscosity. The density and viscosity of the encapsulant will be increase when the filler loading is increase. High density of encapsulant will causing the viscosity of the encapsulant become more viscous, literally will causing the flow of encapsulant will become slower.

Besides, nano silica is carried away that is dispense through continuous phase are follow the encapsulant through the transfer of momentum of encapsulant to the filler particle. With high filler loading mean higher momentum of encapsulant is transfer to the filler particle, causing huge amount of momentum and kinetic energy is lost. Thus, this causing the

filler loading to flow to flow much slower compare to the encapsulant that have low filler loading. Moreover, with high filler loading the encapsulant is exposed to large drag coefficient which dampen the flow.

Next, with higher filler loading the frequency of elastic collisions between solder ball and filler particle is increase. This causing the particle to bounce off during the collision with the solder ball which resulting more dissipation in the kinetic energy of the filler particles. Due to relatively small sizes of filler particle the small change of the velocity will become more prominent. This will reduce the kinetic energy thus the filling time will reduce much more.

Next, the present of the solder ball create cumulative resistance to the flow. The significant impact of solder ball resistance on underfill flow BGA has been demonstrated by Wan et al. analytically [22].

Table 4. 7. Flow front of mixture of encapsulant and 5 wt% filler particles through BGA model at difference thermal energy.

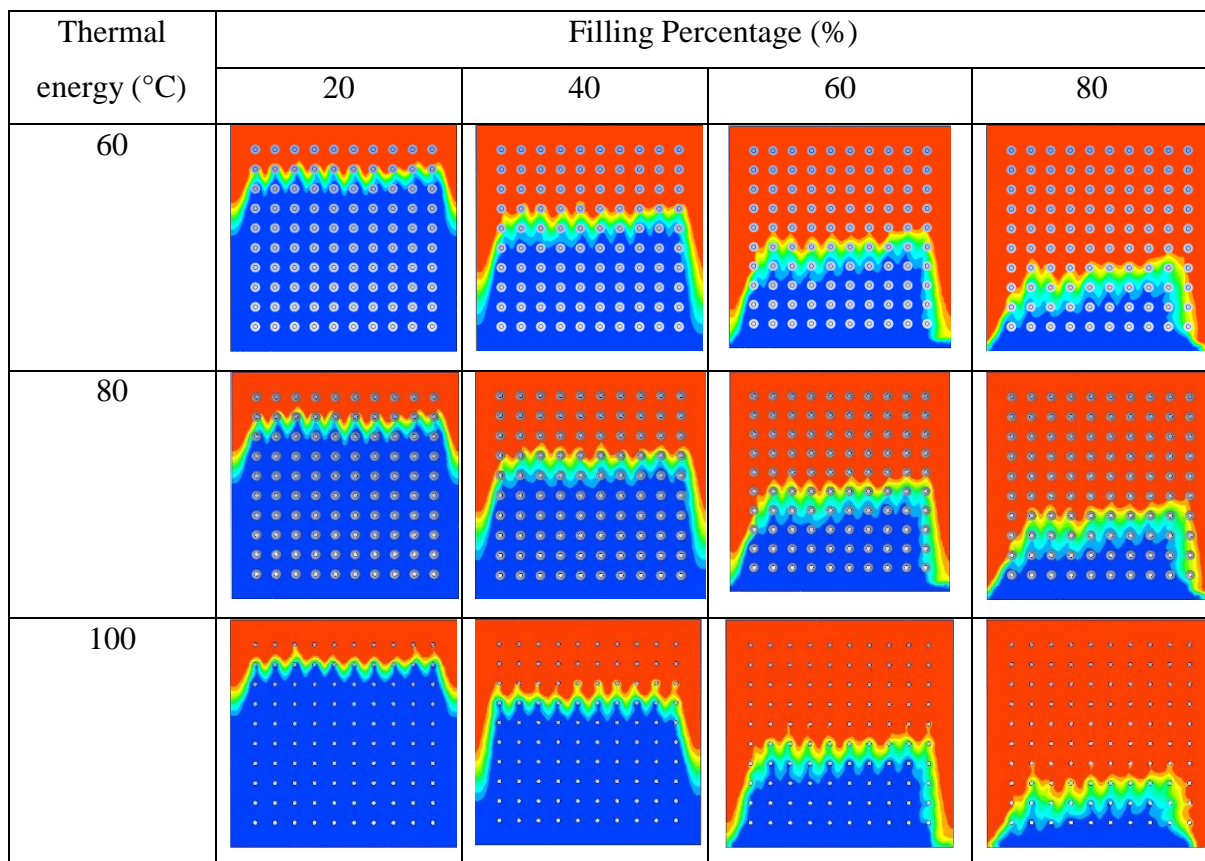


Table 4. 8 Filling time of 5 wt% filler loading at difference thermal Energy

Filling Percentage (%)	Thermal Energy		
	60 °C	80 °C	100 °C
	Filling time (s)		
20	0.5	0.38	0.31
40	1.01	0.96	0.9
60	2.51	2.45	2.4
80	6.1	5.97	5.8

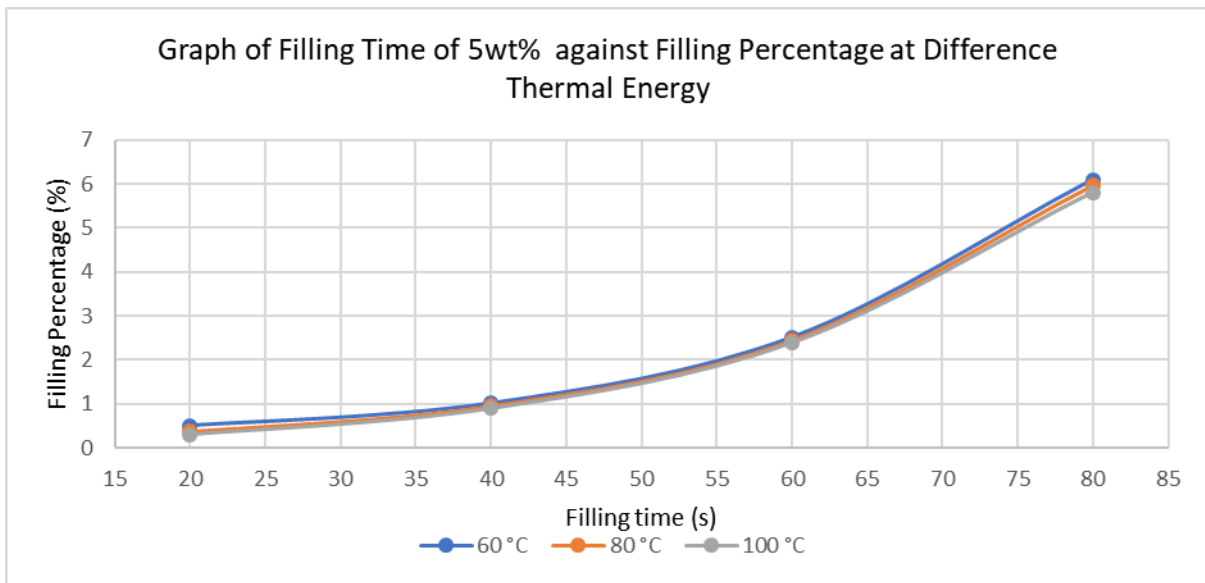
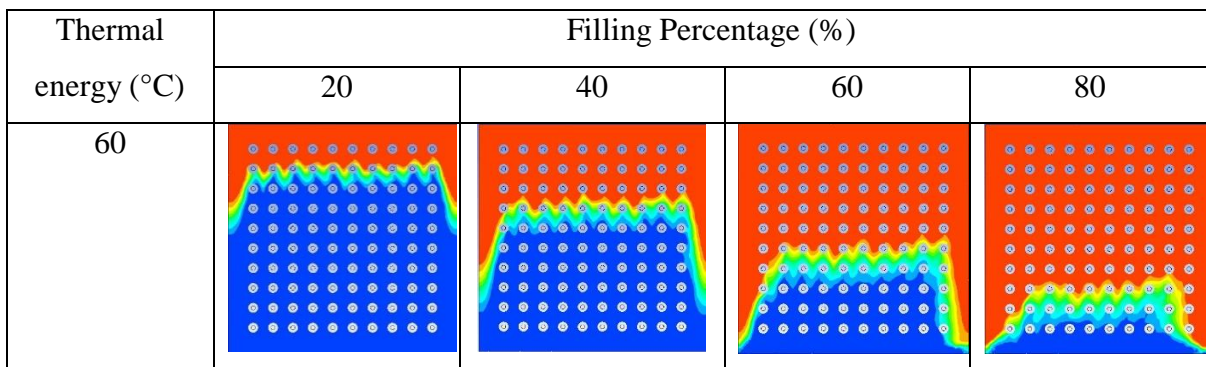


Fig. 4. 3. Show the effect of thermal energy to the filling time of 5 wt% filler loading.

Table 4. 9. Flow front of mixture of encapsulant and 10 wt% filler particles through BGA model at difference thermal energy.



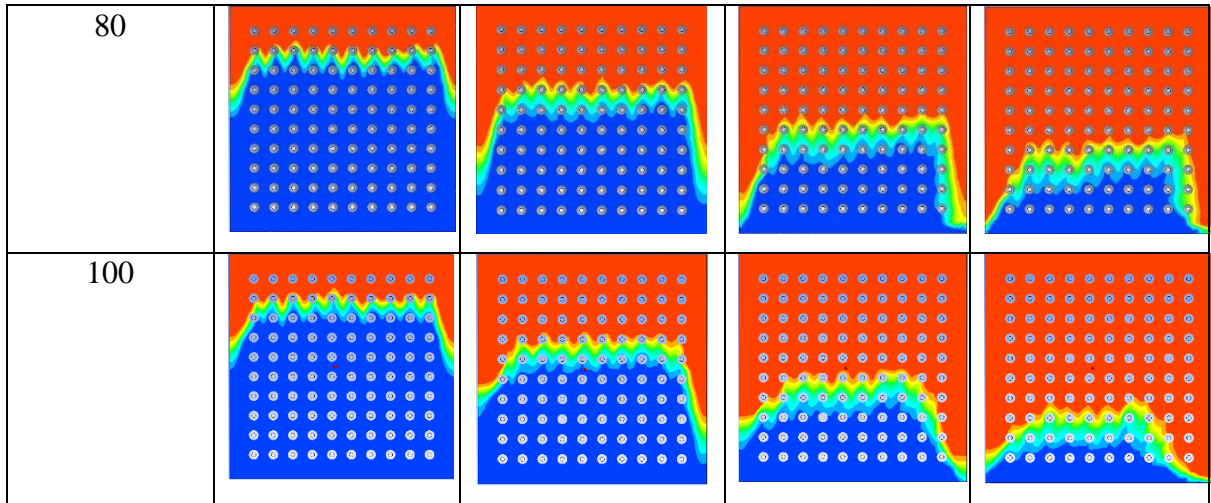


Table 4. 10 Filling time of 10 wt% filler loading at difference thermal Energy

Filling Percentage (%)	Thermal Energy		
	60 °C	80 °C	100 °C
	Filling time (s)		
20	0.63	0.55	0.49
40	1.45	1.23	1.03
60	2.95	2.91	2.64
80	6.4	6.27	6.12

